Dalton Transactions

Polar derivatives of [closo-1-CB9H10]- and [closo-1-CB11H12]- anions as high Δε additives to a nematic host: a comparison of the CH2CH2 and COO linking groups

Journal:	*Dalton Transactions*
Manuscript ID	DT-ART-01-2021-000211.R1
Article Type:	Paper
Date Submitted by the Author:	10-Feb-2021
Complete List of Authors:	Kaszynski, Piotr; Centrum Badan Molekularnych i Makromolekularnych Polskiej Akademii Nauk, Heteroorganic Chemistry; Middle Tennessee State University College of Basic and Applied Sciences, Chemistry Jakubowski, Rafał; Centrum Badan Molekularnych i Makromolekularnych Polskiej Akademii Nauk, Heteroorganic Chemistry Pecyna, Jacek; Middle Tennessee State University College of Basic and Applied Sciences Ali, Muhammad; Middle Tennessee State University College of Basic and Applied Sciences, Chemistry Pietrzak, Anna; Politechnika Łódzka, Institute of Organic Chemistry Friedli, Andrienne; Middle Tennessee State University, Chemistry

ARTICLE

Polar derivatives of [*closo*-1-CB_9H_{10}]$^-$ and [*closo*-1-$CB_{11}H_{12}$]$^-$ anions as high $\Delta\varepsilon$ additives to a nematic host: a comparison of the CH_2CH_2 and COO linking groups†

Received 00th January 20xx,
Accepted 00th January 20xx

DOI: 10.1039/x0xx00000x

Rafał Jakubowski,[a] Jacek Pecyna,[b] Muhammad O. Ali,[b] Anna Pietrzak,[b,c] Andrienne C. Friedli [b] and Piotr Kaszyński [a,b,d]

A series of liquid crystalline pyridinium and sulfonium derivatives of the [*closo*-1-CB_9H_{10}]$^-$ and [*closo*-1-$CB_{11}H_{12}$]$^-$ anions containing the CH_2CH_2 linking group was prepared and their molecular and crystal structures were determined by single crystal XRD methods. Thermal and dielectric properties of the series were evaluated in a weakly polar nematic host. The highest extrapolated dielectric anisotropy, $\Delta\varepsilon$, was observed for pyridinium zwitterions (up to 56.0). The dielectric data were analyzed with the Maier-Meier formalism augmented with density functional theory calculations, and the results were compared to those obtained for the analogous ester derivatives (COO linking group). The effect of the linking group on thermal and electrooptical properties is discussed.

Introduction

Large longitudinal dipole moments of zwitterionic derivatives of the [*closo*-1-CB_9H_{10}]$^-$ (**A**) and [*closo*-1-$CB_{11}H_{12}$]$^-$ (**B**) anions (Fig. 1) make them attractive structural elements for polar liquid crystals[1,2] and additives for use in the liquid crystal display (LCD) industry.[3,4] The molecular dipole moment affects directly the magnitude of dielectric anisotropy, $\Delta\varepsilon$[5] of the liquid crystalline material, which controls the voltage characteristics of the electro-optical switching.[6] In general, the larger $\Delta\varepsilon$, the lower the operational voltage of the device.

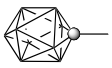

B IIB

Fig. 1. Structures of the [*closo*-1-CB_9H_{10}]$^-$ and [*closo*-1-$CB_{11}H_{12}$]$^-$ anions (**A** and **B**) and their zwitterionic derivatives (**I** and **II**). Each vertex represents a BH fragment, the sphere is a carbon atom, and Q^+ stands for an onium group (sulfonium or pyridinium).

In the context of developing new materials for LCD applications, we have investigated liquid crystalline esters **IA** and **IB** (Fig. 1) as highly polar, low concentration additives to nematic hosts.[7-10] Results demonstrated that some of the esters exhibit a dielectric anisotropy ($\Delta\varepsilon$) as high as 113.[7,8] Unfortunately, esters generally increase the viscosity of the material, which affects device switching times.[2,6] In order to improve molecular parameters and also to increase hydrolytic stability of the polar additives, we have focused on analogues **II** (Fig. 1), in which an ester linker is replaced with a CH_2CH_2 group.

Herein we report the preparation and XRD studies of two series of derivatives of type **II**: pyridinium and sulfonium zwitterions **1[n]** and **2[3]b**, respectively, of the [*closo*-1-CB_9H_{10}]$^-$ and [*closo*-1-$CB_{11}H_{12}$]$^-$ anions (Fig. 2). The derivatives were investigated for their thermal behavior and as low concentration additives to a nematic host. The binary mixtures were studied by thermal and dielectric methods. The dielectric results were analyzed using the Maier-Meier formalism, which

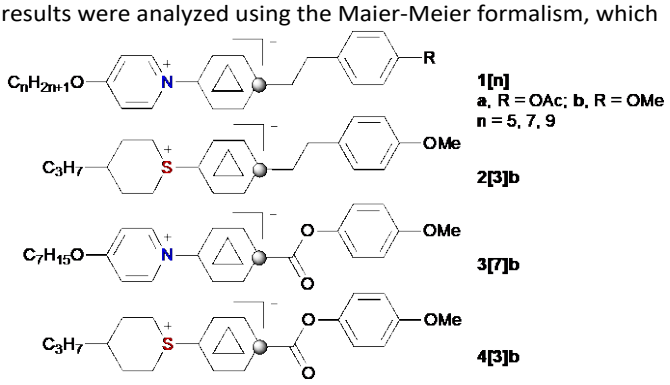

Fig. 2. Structures of derivatives **1[n]** – **4[3]b**. The central ring represents either the substituted [*closo*-1-CB_9H_{10}]$^-$ (series **A**) or [*closo*-1-$CB_{11}H_{12}$]$^-$ (series **B**). See Fig. 1.

[a] *Centre of Molecular and Macromolecular Studies, Polish Academy of Sciences, 90-363 Łódź, Poland*
[b] *Department of Chemistry, Middle Tennessee State University, Murfreesboro, TN, 37130, USA.*
[c] *X-ray Crystallographic Laboratory, Department of Chemistry, Łódź Technical University, 90-924 Łódź, Poland*
[d] *Faculty of Chemistry, University of Łódź, 91-403 Łódź, Poland*

† Electronic Supplementary Information (ESI) available: NMR spectra, DSC traces, thermal and dielectric data for binary mixtures, Maier-Meier analysis details, DFT results, and archive of calculated equilibrium geometries for **1[n]**–**4[n]**. This material is available free of charge via the Internet at. See DOI: 10.1039/x0xx00000x

relates molecular parameters, derived from DFT calculations, and experimental bulk parameters of the additive. The results for compounds of type **IIA** were compared to those of the isostructural esters **3A[7]b** and **4A[3]b** (Fig.2).

Results and discussion

Synthesis

Preparation of pyridinium and sulfonium derivatives (**1[n]** and **2[3]b**) took advantage of our recently developed synthetic access to functional intermediates **5A** and **5B** (Scheme 1),[11] in which the phenyliodonium substituent serves as a convenient and effective leaving group in the 10-I-3 nucleophilic substitution process.[12] Thus, the reaction of **5a** with 4-alkoxypyridines[13] **6[n]** led to the corresponding pyridinium zwitterions **1[n]a** isolated in 87–89% yield. A similar reaction of **5b** with 4-heptyloxypyridine[13] (**6[7]**) gave **1[7]b** in comparable yields.

Synthesis of the sulfonium derivatives **2A[3]b** and **2B[3]b** was a two-step process as shown in Scheme 1. Thus, a reaction of phenyliodonium **5b** with Me_2NCHS gave the protected mercaptan **7b**, which was cycloalkylated with 1,5-dibromo-3-propylpentane[14] (**8**) under basic and hydrolytic conditions.[15] The resulting sulfonium zwitterion **2[3]b** was isolated in an overall yield of about 70%.

Scheme 1 Synthesis of zwitterions **1[n]** and **2[3]b**.[a]

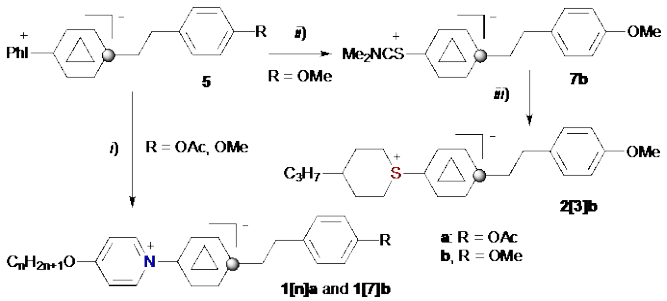

[a] *Reagents and conditions*: *i*) 4-$C_nH_{2n+1}OC_5H_4N$ (**6[n]**), 85 °C, 6h or **6[n]** (5 equiv), CH_2Cl_2, 50 °C, 16h; *ii*) Me_2NCHS, 100 °C, 1h; *iii*) $C_3H_7CH(CH_2CH_2Br)_2$ (**8**), $[NMe_4]^+OH^- \bullet 5H_2O$, MeCN, rt, 12h.

Scheme 2 Synthesis of zwitterions **3A[7]b** and **4A[3]b**.[a]

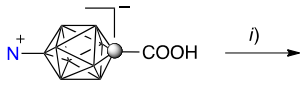

[a] *Reagents and conditions*: *i*) 1. $(COCl)_2$, DMF (cat.), CH_2Cl_2, rt, 1h; 2. 4-$MeOC_6H_4OH$, Et_3N, CH_2Cl_2, rt, 1h.

Esters **3A[7]b** and **4A[3]b** were obtained from the previously reported carboxylic acids **9A[7]** [7,12] and **10A[3]**,[9,16] respectively, according a general literature procedure[16] (Scheme 2). The analogous ester of the carbaborate **B** could not be obtained due to the lack of the appropriate carboxylic acids.

^{1}H NMR analysis revealed that sulfonium zwitterions **2[3]b** and **4[3]b** exist as mixtures of interconverting epimers, *trans* and *cis* isomers, in the ratio of about 3:1 for derivatives of anion **A** and about 5:1 for those anion **B** (Fig. 3). This is consistent with our previous findings[9,17] and the results of DFT calculations.[17]

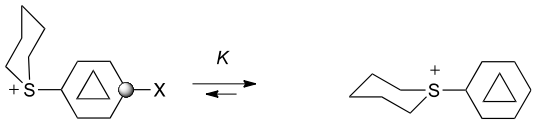

Fig. 3. Epimerization at the sulfur center in sulfonium derivatives **2** and **4**.

Crystal and molecular structures

Colorless monoclinic crystals of **1A[7]b**, **1B[7]b**, and **2A[3]b** and triclinic crystals of **2B[3]b** were obtained by slow cooling of AcOEt/*i*-octane solutions. Their solid-state structures were determined by low temperature single crystal X-ray analysis and the results are shown in Table 1 and in Figs. 4 and 5. Full details of data collection and refinement are provided in the ESI.

Crystal systems of **1B[7]b** and **2A[3]b** contain a single molecule in the asymmetric unit and four molecules in the unit cell, while two and three molecules are found in the asymmetric unit of **1A[7]b** and **2B[3]b**, respectively.

Table 1. Selected interatomic distances and angles for derivatives **1[7]b** and **2[3]b**.

	1A[7]b [a]	1B[7]b	2A[3]b	2B[3]b [b]
X–B(10/12)	1.520(4)	1.544(1)	1.857(2)	1.895(4)
C(1)–CH_2	1.510(4)	1.532(1)	1.517(2)	1.533(2)
CH_2–CH_2	1.526(4)	1.533(2)	1.534(2)	1.524(4)
CH_2–C_{Ph}	1.511(4)	1.512(1)	1.514(2)	1.510(3)
C(1)···B(10/12)	3.512(4)	3.221(1)	3.507(2)	3.208(4)
L core [c]	14.28	13.989(1)	14.457(2)	14.29(9)
C(1)–C–C	113.8(2)°	116.4(1)°	115.1(1)°	115°
Ph/CH_2CH_2 [d]	60.0/49.3°	67.3(1)°	66.2°	65.3/80.9/88.8°
Ph/OCH_3 [e]	3.3/13.7°	11.9(1)°	4.0°	1.9/14.6/3.0°
cage/CH_2CH_2 [f]	0.5/14.2°	14.0°	8.7°	0.9/34.0/29.9°
cage/ring [g]	9°	12.8°	21.9°	15.6/10.3/10.2°

[a] Two unique molecules. [b] Three unique molecules. [c] Length of the core defined as C_{ring}···C_{Ph}. [d] Angle between Ph ring and C–CH_2CH_2–C planes. [e] C–C–O–Me angle. [f] Angle from the ideal staggered conformation.

Dimensions of the boron cages, benzene and heterocyclic rings in derivatives **1[7]b** and **2[3]b** (Table 1 and Fig. 4) are typical for similar C-alkyl,[11,18-20] B-sulfonium[21] and B-pyridinium[21-23] derivatives of the [*closo*-1-CB_9H_{10}]$^-$ [11,18,21-23] and [*closo*-1-$CB_{11}H_{12}$]$^-$ [11,19,20,23] anions and analogous zwitterionic derivatives of [*closo*-$B_{10}H_{10}$]$^{2-}$ [24-26] and [*closo*-$B_{12}H_{12}$]$^{2-}$.[24,27] The length *L* of the molecular core, consisting of the heterocyclic ring, boron cage and the phenethyl substituent is about 14 Å (Table 1). The core is slightly longer for derivatives of cluster **A** than in analogues of cluster **B** and for sulfonium **2[3]** than for

pyridinium derivatives **1[7]**. The CH_2CH_2 group and heterocyclic rings typically adopt an orientation relative to the boron cage that is close to a staggered conformation. Typically, the CH_2CH_2 group is oriented at about 60° with respect to the benzene ring. In one molecule of **2B[3]b** this orientation is nearly orthogonal.

The heptyl chain in the pyridinium derivatives adopts a single gauche conformation at C(2)–C(3) (**1A[7]b**, molecule A), C(1)–C(2) (**1B[7]b**) or a double gauche at C(2)–C(3) and C(5)–C(6) (**1A[7]b**, molecule B). The propyl chain in the sulfonium derivatives is oriented *anti* to the C(4)–C(3) bond in the 6-membered ring. In **2A[3]b** the propyl chain is positionally disordered over two sites.

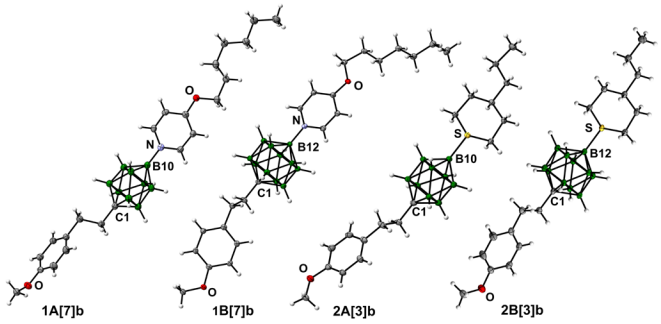

Fig. 4. Atomic displacement ellipsoid representation of **1A[7]b**, **1B[7]b**, **2A[3]b** and **2B[3]b**. For geometrical dimensions see Table 1 and the text. The corresponding ellipsoids are at the 50% probability level and the numbering system according to the chemical structure.

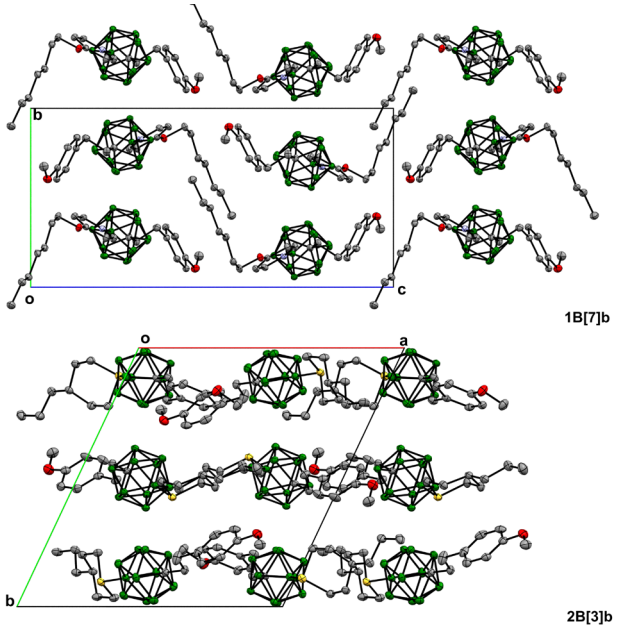

Fig. 5. Crystal packing of **1B[7]b** and **2B[3]b**. Hydrogen atoms are omitted for clarity.

Molecules of **1A[7]B** and **1B[7]b** form intermolecular hydrogen bonds between the C-H group of the pyridine ring and oxygen atom of the methoxy group. The O···H contact distances are 0.105 Å and 0.087 Å shorter than the sum of the van der Waals (vdW) radii, respectively. All investigated crystal structures are characterized by short C-H···B contacts. In **1B[7]b**, these interactions are complemented by a C-H···π contact (0.105 Å inside the vdW separation) between the alkyl chain and phenyl ring of the neighboring molecules. Supramolecular packing of all studied compounds may be presented as boron cages assembled in layers parallel to the (*010*) plane (Fig. 5).

Liquid crystalline properties

Thermal behavior of compounds **1[n]**–**4A[3]b** was investigated by differential scanning calorimetry (DSC) and polarized optical microscopy (POM). The results are shown in Tables 2–4 and Figs. 6 and 7.

All pyridinium derivatives exhibit exclusively nematic behavior with melting temperatures in the range of 100–200 °C and clearing temperatures as high as 231 °C (**1B[5]a**, Table 1, Fig. 6). Most of the compounds also exhibit crystalline polymorphism. A detailed comparison shown in Fig. 7 demonstrates that the acetoxy derivatives of the [*closo*-1-$CB_{11}H_{12}]^-$ anion (series **B**) have higher transition temperatures, both melting and nematic-isotropic (N–I), than the [*closo*-1-$CB_9H_{10}]^-$ analogues in series **A**, and the difference diminishes from 35 K for the **1[5]a** pair to 24 K for the **1[9]a** pair. These findings are consistent with general trends for mesogenic derivatives of *closo*-boranes, which are related to the symmetry of the clusters and conformational space of their substituents, hence overall dynamic anisometry of the molecules.[1] A comparison of **1[7]a** with **1[7]b** demonstrates that the former derivatives with the OAc terminal group have higher N-I transition temperatures than the OMe analogues, which is in agreement with general trends in liquid crystals.[28] Further analysis indicates that the methoxy derivatives in series **A** with the CH_2CH_2 linker exhibit higher transition temperatures, for both melting and clearing, than the ester analogues (Tables 3 and 4). The observed higher stability of the nematic phase in **1A[7]b** than in **3A[7]b** is contrary to expectations based on results for a series of [*closo*-1,12-$C_2B_{10}H_{12}$] derivatives,[29] which is presumably related to stronger dipolar interactions in the present series.

Table 2. Transition temperatures (°C) and enthalpies (kJ/mol, in italics) for **1[n]a**. [a]

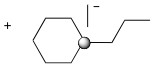

1[n]a

n	A	B
5	Cr_1 133 (*19.4*) Cr_2 156 (*17.8*) N 196 (*2.1*) I	Cr_1 129 (*9.2*) Cr_2 184 (*19.1*) N 231 (*2.4*) I
7	Cr 142 (*23.0*) N 176 (*3.0*) I [N 140±2 I][b]	Cr 173 (*32.4*) N 205 (*1.8*) I [N 138 I][c]
9	Cr_1 71 (*17.1*) Cr_2 132 (*14.9*) N 163 (*2.1*) I	Cr_1 145 (*11.1*) Cr_1 149 (*14.5*) N 187 (*1.7*) I

[a] Peak of transition determined by DSC in the heating mode: Cr = crystal; N = nematic; I = isotropic. Heating rate 10 K min^{-1}. [b] Virtual transition temperature [T_{NI}] extrapolated from solutions in **ClEster**. [c] Virtual T_{NI} transition temperature extrapolated from 4.2 mol% solution in **ClEster.**

Sulfonium derivatives **2A[3]b** and **4A[3]b** have high melting points and exhibit monotropic nematic phases in significantly supercooled liquids (Table 4). Similarly to pyridinium

derivatives, **2A[3]b** with the CH_2CH_2 linking group exhibits higher stability of the nematic phase than the ester analogue **4A[3]b**. In contrast, **2B[3]b** has a narrow range enantiotropic nematic phase with a clearing temperature of 214 °C.

Table 3. Transition temperatures (°C) and enthalpies (kJ/mol, in italics) for pyridinium derivatives **1[7]b** and **3A[7]b**. [a]

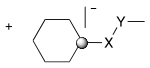

	X–Y	A	B
1[7]b	CH_2CH_2	Cr 136 (*27.0*) N 168 (*0.8*) I [N 130±2 I] [b]	Cr 165 (*21.8*) N 200 (*1.4*) I [N 142±1 I] [b]
3[7]b	COO	Cr 133 (*20.0*) N 163 (*1.2*) I [N 115±2 I] [b]	–

[a] Peak of transition determined by DSC in the heating mode: Cr = crystal; N = nematic; I = isotropic. Heating rate 10 K min^{-1}. [b] Virtual transition temperature [T_{NI}] extrapolated from solutions in **ClEster**.

Table 4. Transition temperatures (°C) and enthalpies (kJ/mol, in italics) for sulfonium derivatives **2[3]b** and **4A[3]b**.[a]

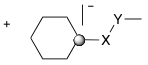

	X–Y	A	B
2[3]b	CH_2CH_2	Cr 184 (*33.4*) (N 150) [b] I [N 115±4 I] [c]	Cr 207 (*22.9*) N 214 (*1.5*) I [N 174 I] [d]
4[3]b	COO	Cr 166 (34.4) (N 106) [b] I [N 100±1 I] [c]	–

[a] Peak of transition determined by DSC in the heating mode: Cr = crystal; N = nematic; I = isotropic. Heating rate 10 K min^{-1}. [b] Monotropic transition observed on cooling on a hot stage. [c] Virtual transition temperature [T_{NI}] extrapolated from solutions in **ClEster**. [d] Virtual T_{NI} transition temperature extrapolated from 1.8 mol% solution in **ClEster**.

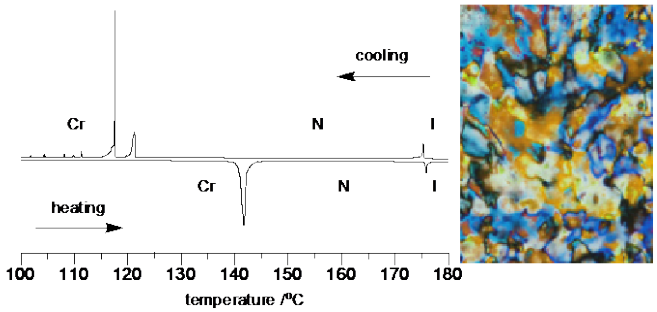

Fig. 6. Left: DSC trace of **1A[7]b**. The heating and cooling rates are 10 K min^{-1}. Right: The optical texture of **1A[7]b** obtained at 150 °C on cooling from the isotropic phase.

Binary mixtures

To assess suitability of the zwitterions for electrooptical applications, all derivatives were investigated as low concentration additives to **ClEster**, which is an ambient temperature nematic with a small negative dielectric anisotropy, $\Delta\varepsilon = -0.56$.[30,31]

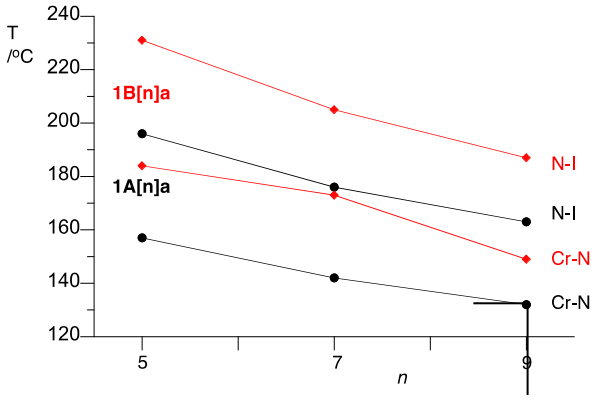

Fig. 7. Phase diagram for homologous series **1A[n]a** (black circles) and **1B[n]a** (red diamonds): Cr-crystalline, N-nematic, I-isotropic. The lines are guides for the eye.

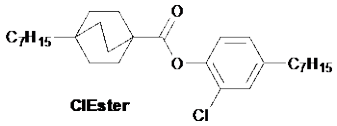

ClEster

Thermal analysis of binary mixtures revealed a stabilizing effect for all additives on the nematic phase of the host. The linear dependence of the T_{NI} on concentration, indicating ideal behavior of the solutions, was observed in a full range of concentrations (up to 12 mol%) only in the case of pyridinium derivatives **1[7]b** and **3A[7]b** (Fig. 8). The acetoxy analogues **1A[7]a** and **1B[7]a** exhibited lower compatibility with the host and the linear dependence on concentration was observed up to 8 and 4 mol%, respectively. The lowest solubility in **ClEster** was observed for the sulfonium derivatives **2[3]b** and **4A[3]b** (<5 mol%), which results in nonlinear behavior of the $T_{NI}(x)$ plot (Fig. 8). Overall, slow partial crystallization was observed at ambient temperature for concentrations above 4 mol% in nearly all mixtures with the exception of **1A[7]b**, for which crystals appeared only in a 12 mol% solution.

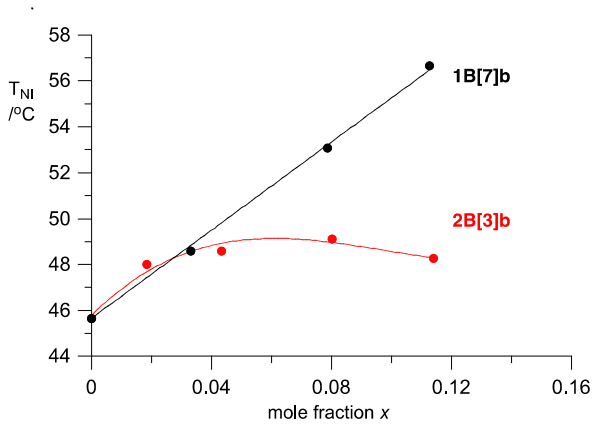

Fig. 8. Peak temperature of the N–I transition for binary mixtures of **1B[7]b** (black) and **2B[3]b** in **ClEster**.

The extrapolated virtual N–I transition temperatures [T_{NI}] for all 8 derivatives range from 100±1 °C for **4A[3]b** to 174 °C

for **2B[3]b** (Tables 2–4). A comparison of the clearing temperatures demonstrates that the extrapolated values [T_{NI}] are typically lower than those measured for pure compounds by about 40 K, with the exception of **4A[3]b** for which the difference is much smaller.

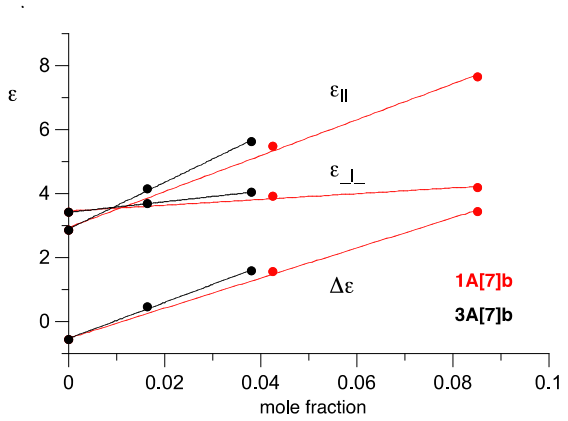

Fig. 9. Dielectric parameters as a function of concentration of **1A[7]b** (red) and **3A[7]b** (black) in **ClEster**.

Homogenous binary mixtures were analyzed in 12 μm, planar electrooptical cells at *ca*. 22 °C, and dielectric permittivity parallel (ε_{II}) and perpendicular ($\varepsilon_{\perp}$) to the main molecular axes and also dielectric anisotropy ($\Delta\varepsilon = \varepsilon_{II} - \varepsilon_{\perp}$) were measured for 6 additives at concentrations typically below 4 mol%. Only in the case of **1A[7]b** and **1B[7]b** did solubility permit analysis of 8 mol% mixtures. For additives **1A[7]a**, **1A[7]b**, **1B[7]b** and **3A[7]b** results for two concentrations were obtained, which along with the datapoints for the pure host gave a linear dependence of dielectric parameters, ε_{II}, $\varepsilon_{\perp}$, and $\Delta\varepsilon$ on concentration (Fig. 9). Extrapolation of the values to 100 mol% gave dielectric parameters for pure additives shown in Table 5. For sulfonium derivatives **2B[3]b** and **4A[3]b** dielectric parameters were obtained from a single concentration (and data for the pure host), while derivatives **1B[7]a** and **2A[3]b** could not be analyzed due to rapid crystallization of even 4 mol% solutions.

Analysis of dielectric parameters for pure additives collected in Table 5 demonstrates three trends towards higher dielectric anisotropy Δε: pyridinium zwitterions **1[7]** and **3[7]** exhibit higher Δε than the sulfonium derivatives **2[3]b** and **4[3]b**, zwitterions with the COO linking group (**3[7]b** and **4[3]b**) have higher Δε than those with the CH_2CH_2 linker (**1[7]b** and **2[3]b**), and compounds wit the acetate group have higher Δε than those with OMe (**1A[7]a** *vs* **1A[7]b**). The highest extrapolated Δε values (56.0) were obtained for **1A[7]a** and **3A[7]b**, while the lowest were observed for **2B[3]b** (Δε = 26.0). Overall, the effectiveness of the additives in boosting dielectric anisotropy Δε of the mixture increases in the order: **2B[3]b** < **4A[3]b** < **1B[7]b** < **1A[7]b** < **1A[7]a** ≈ **3A[7]b**.

Measurements in the electrooptical cells also permitted evaluation of the main elastic constants of the nematic material, splay, twist and bend (K_{11}, K_{22}, and K_{33}, respectively) and rotational viscosity γ for **1A[7]b**, **1B[7]b** and **3A[7]b**. Analysis of the results demonstrates that the first two derivatives, **1A[7]b** and **1B[7]b**, systematically increase splay and twist constants, K_{11} and K_{22}, while the bend constant K_{33} decreases with increasing concentration of the polar additive. Consequently, the K_{33}/K_{11} ratio decreases with increasing concentration (Fig. 10). These results are consistent with increasing dipolar intermolecular interactions in the solutions. The increasing values of the elastic constants K_{11} and K_{22} suggest that the molecules are more difficult to separate (more "sticky"). The decreasing K_{33} constant indicates close contacts of local dipole moments and better overlap of rigid cores leading to uneven distribution of rigid and flexible molecular fragments in the material, and consequently easier bending in the aliphatic chain-rich sections of the material. This molecular distribution is a form of molecular aggregation.

Further analysis indicates that both **1A[7]b** and **1B[7]b** increase rotational viscosity of the mixture, with the former additive having a larger effect on γ.[32] Thus for about 3.8 mol% the measured γ is 114 and 96 mP for solutions of **1A[7]b** and **1B[7]b**, which compares to 185 mP measured for the ester analogue **3A[7]b**.

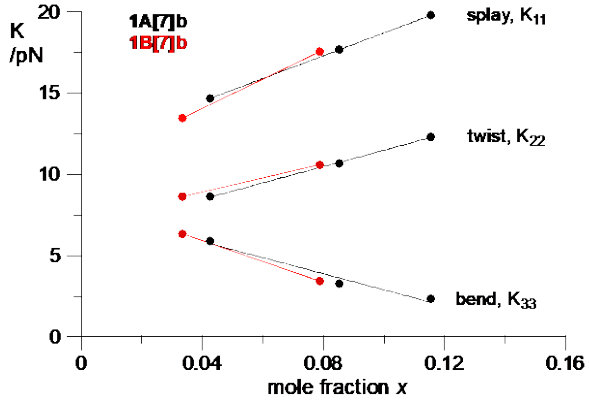

Fig. 10. Elastic constants as a function of the mole fraction of **1A[7]b** (black) and **1B[7]b** (red) in **ClEster**.

Dielectric data analysis

Extrapolated dielectric parameters in Table 5 were analyzed by using the Maier–Meier relationship[33] (eq. 1), which connects molecular and phase parameters.[5] By using experimental ε_{II} and Δε values and DFT-calculated parameters μ, α, and β (Table 6), equations 2 and 3 were used to calculate the apparent order parameter S_{app} [34] and the Kirkwood factor $g = (\mu_{eff}/\mu)^2$ (Table 5). The effect of the additive was ignored in the determination of field parameters *F* and *h* in eq. 2 and 3; *F* and *h* were calculated by using the experimental dielectric and optical data for pure **ClEster** host.[35]

$$\Delta\varepsilon = \frac{NFh}{\varepsilon_0}\left\{\Delta\alpha - \frac{F\mu_{eff}^2}{2k_BT}(1-3cos^2\beta)\right\}S \qquad \text{eq 1}$$

$$S = \frac{2\Delta\varepsilon\varepsilon_0}{NFh[2\Delta\alpha+3\bar{\alpha}(1-3cos^2\beta)]-3(\bar{\varepsilon}-1)\varepsilon_0(1-3cos^2\beta)} \qquad \text{eq 2}$$

$$g = \frac{[(\varepsilon_{\parallel}-1)\varepsilon_0-\bar{\alpha}NFh-\frac{2}{3}\Delta\alpha NFhS]3k_BT}{NF^2h\mu^2[1-(1-3cos^2\beta)S]} \qquad \text{eq 3}$$

The molecular electric dipole moment μ and polarizability α required for the analysis were obtained at the B3LYP/6-31+G(2d,p)//B3LYP/6-31G(2d,p) level of theory in the dielectric medium of **ClEster**.[32] Molecular parameters of configurationally mobile sulfonium zwitterions **2[3]b** and **4[3]b** (Fig. 3) were established as a weighted sum of parameters of individual *trans* and *cis* isomers in 78.5 to 21.5 ratio for series **A** [9] and 89 to 11 for series **B**.[17] Since not all additives could be analyzed in the nematic host, for comparison purposes the behavior of the missing members of the series was also evaluated using assumed values *S* and *g* (Table 5, in italics) and DFT derived molecular parameters.

Table 5. Extrapolated experimental (upper) and predicted (lower, in italics) dielectric data and results of Maier-Meier analysis for selected compounds.[a]

Compound	$\varepsilon_{\parallel}$	$\varepsilon_{\perp}$	$\Delta\varepsilon$	S_{app}	g
1A[7]a	69.8	13.8	56.0	0.64	0.41
	85.7	*15.9*	*69.0*	*0.65*[b]	*0.50*[b]
1A[7]b	60.1	13.0	47.1	0.61	0.38
	80.2	*14.9*	*65.4*	*0.65*[b]	*0.50*[b]
1B[7]a	[c]	[c]	[c]	[c]	[c]
	76.2	*14.6*	*61.6*	*0.65*[b]	*0.50*[b]
1B[7]b	53.0	12.5	40.5	0.59	0.39
	69.9	*13.3*	*56.6*	*0.65*[b]	*0.50*[b]
2A[3]b	[c]	[c]	[c]	[c]	[c]
	45.4	*10.4*	*35.0*	*0.65*[b]	*0.50*[b]
2B[3]b [d]	36.9	10.9	26.0	0.55	0.50
	39.8	*9.3*	*30.5*	*0.65*[b]	*0.50*[b]
3A[7]b [d]	75.9	19.9	56.0	0.58	0.42
	94.3	*20.4*	*73.9*	*0.65*[b]	*0.50*[b]
3B[7]b	[c]	[c]	[c]	[c]	[c]
	74.7	*16.6*	*58.1*	*0.65*[b]	*0.50*[b]
4A[3]b	51.0	17.2	33.8	0.50	0.58
	50.6	*12.4*	*38.3*	*0.65*[b]	*0.50*[b]
4B[3]b	[c]	[c]	[c]	[c]	[c]
	41.8	*11.4*	*30.4*	*0.65*[b]	*0.50*[b]

[a] Typical uncertainty of the measured values is about 0.1. For details see text and ESI. [b] Assumed value. [c] Not measured. [d] Extrapolated from data for the host and ~4 mol% solution.

Analysis of S_{app} and g parameters obtained from extrapolated values $\Delta\varepsilon$ and ε_{II} and equations 2 and 3 demonstrates that all six additives are compatible with the nematic host in low concentrations. The apparent order parameter S_{app}, which provides information on alignment of the additive with the nematic director, is above 0.50 (Table 5). The highest values were obtained for **1A[7]a** (S_{app} = 0.64) and **1A[7]b** (S_{app} = 0.64), which are close to that for the pure host (S = 0.67 at 22 °C).[31] For comparison, S_{app} is slightly lower for the ester analogue **3A[7]b** (0.58). Not surprisingly, the lowest S_{app} values were obtained for the sulfonium derivatives. The second parameter, Kirkwood factor g is typically around 0.4 for pyridinium derivatives (Table 5) and higher for sulfonium **2B[3]b** (g = 0.50) and **4A[3]b** (g = 0.58) indicating a low degree of association in solution (which is consistent with the linear behavior of the parameters as function of concentration for these compounds).

Analysis of DFT the results in Table 6 demonstrates that pyridinium derivatives **1[7]**, in which the positive charge is delocalized in the heterocyclic ring, have large electric dipole moment μ (13–15 D) oriented nearly parallel to the long molecular axis (small $\mu_{\perp}$ and β). The sulfonium derivatives exhibit smaller net dipole moments by about 5 D and higher angles β. Replacement of the COO group with the CH_2CH_2 linker in series **1[7]** slightly decreases dipole moment in **3[7]**, typically by about 1 D. These trends are consistent with those in experimental $\Delta\varepsilon$ values in Table 5.

Table 6. Calculated molecular parameters for selected compounds. [a]

Compd	$\mu\vert\vert$ /D	$\mu_{\perp}$ /D	μ /D	β[b] /°	$\Delta\alpha$ /Å^3	α_{avrg} /Å^3
1A[7]a	14.74	1.72	14.84	6.6	45.85	71.59
1A[7]b	13.81	1.24	13.86	5.1	44.02	69.35
1B[7]a	14.20	1.99	14.34	8.0	42.34	73.76
1B[7]b	13.18	1.17	13.24	5.1	40.30	71.51
2A[3]b[c]	9.60	2.11	9.83	12.4	30.69	61.15
2B[3]b	9.21	1.91	9.41	11.7	29.52	63.83
3A[7]b	15.22	4.20	15.79	15.5	44.87	68.49
3B[7]b	13.83	3.84	15.53	15.5	41.77	70.61
4A[3]b[c]	10.36	3.16	10.84	17.0	33.48	60.28
4B[3]b	9.59	3.46	10.19	19.9	31.59	62.79

[a] Values obtained at the B3LYP/6-31+G(2d,p)//B3LYP/6-31G(2d,p) level of theory in **ClEster** dielectric medium. [b] Angle between the net dipole vector μ and $\mu_{\parallel}$. [c] Composite molecule 78.5% of *trans* and 21.5% of *cis* for series **A** and 89% of *trans* and 11% of *cis* for series **B**. For details see text and the ESI.

According to the Maier–Meier relationship, expected dielectric anisotropies $\Delta\varepsilon$ are in the range of 56–74 (ε_{II} = 69-94) for the series of pyridinium zwitterions in **ClEster** medium and 30–38 (ε_{II} = 39–51) for the series of sulfonium, assuming a typical order parameter of S = 0.65 and a Kirkwood factor g = 0.50 and taking DFT derived calculated molecular parameters α, β, and μ. A comparison of the predicted and experimental (extrapolated) dielectric parameters for the zwitterions shows that extrapolated values are about 25% larger on average, due to generally lower-than-assumed parameters S and g in solutions. Maier-Meier analysis of the experimental data shows that the apparent order parameter S_{app} is similar (S_{app} in the range of 0.58–0.61) to the pure host (S = 0.67 at 22 °C)[31] for pyridinium derivatives, indicating good alignment of the additive in the host. For comparison, the degree of alignment

for sulfonium derivatives is smaller (S_{app} in a range of 0.5–0.55).

Conclusions

A series of polar nematic liquid crystals, zwitterionic derivatives of [*closo*-1-CB_9H_{10}]$^-$ and [*closo*-1-$CB_{11}H_{12}$]$^-$ anions, was conveniently obtained using recently developed new difunctional building blocks. Analysis of limited examples demonstrate that AcO derivatives **1[7]a** have lower solubility than the MeO analogues **1[7]b**, and sulfonium derivatives **2[3]b** are less soluble than pyridinium **1[7]b** in the **ClEster** host. A comparison of the clearing temperatures for neat compounds and binary mixtures with **ClEster** indicates a stabilizing effect of the CH_2CH_2 linker on the nematic phase relative to the COO group.

Data extrapolated from solutions in **ClEster** demonstrate higher dielectric anisotropy $\Delta\varepsilon$ for derivative **1A[7]b** than **1B[7]b**, which is consistent with the general trend in values predicted on the basis of DFT-calculated molecular parameters (μ, α, β) and assumed ideal bulk behavior (S_{app} and g). This, in turn, results from slightly higher molecular dipole moment μ and anisotropy of polarizability $\Delta\alpha$ for the 10-vertex derivatives in series **A**. A comparison of the CH_2CH_2 and COO linkers demonstrates higher $\Delta\varepsilon$ values for the latter series resulting from higher longitudinal dipole moments. On the other hand, a comparison of the limited data indicates smaller increase of material's viscosity for the CH_2CH_2 containing linking group (**1A[7]b**) than for the analogous ester (**3A[7]b**).

Overall, the additives with the best performance are the pyridinium derivatives in series **A**, either the acetate **1A[7]a** ($\Delta\varepsilon$ = 56.0, S_{app} = 0.64 and g = 0.41) or the ester **3A[7]b** ($\Delta\varepsilon$ = 56.0, S_{app} = 0.58 and g = 0.42).

The presented results suggest that further improvements in the properties are needed, especially better solubility and higher magnitude of dielectric anisotropy. The former can be accomplished by lowering the melting point and extending or adding branched alkyl chains. Increase of the $\Delta\varepsilon$ requires other polar terminal groups, such as OCF_3 or OCH_2CF_3.

Computational Details

Quantum-mechanical calculations were carried out using the Gaussian 09 suite of programs.[36] Geometry optimizations for unconstrained conformers in most extended molecular shapes were undertaken at the B3LYP/6-31G(2d,p) level of theory using default convergence limits. Vibrational frequencies were used to characterize the nature of the stationary points and to obtain exact polarizabilities in vacuum. Dipole moments and exact electronic polarizabilities of selected compounds for use in the Maier–Meier data analysis were obtained in **ClEster** dielectric medium using the B3LYP/6-31+G(2d,p)//B3LYP/6-31G(2d,p) method and the PCM solvation model[37] requested with SCRF(Solvent=Generic, Read) keywords and "eps=3.07" and "epsinf=2.286" parameters (single point calculations). Exact polarizabilities were obtained with the POLAR keyword. Details are provided in the ESI.

Experimental

General. Reactions were conducted in an argon atmosphere and subsequent manipulations in air. TLC analyses were conducted on silica gel plates 60-F254. Column chromatography was performed using 70-230 mesh silica gel (Merck). Melting points were recorded in capillary tubes and are uncorrected. NMR spectra were obtained at 500 MHz (^{1}H), 126 MHz (^{13}C) and 160 MHz (^{11}B) in $CDCl_3$, unless specified otherwise. Chemical shifts were referenced to the solvent ($CDCl_3$: 7.26 ppm for ^{1}H and 77.16 ppm for ^{13}C) [38] and to an external sample of neat BF_3•Et_2O in $CDCl_3$ (^{11}B, δ = 0.0 ppm). ^{11}B NMR chemical shifts were taken from the H-decoupled spectra. HR mass spectrometry was conducted with the TOF-MS ES method typically in the positive mode. Optical microscopy and phase identification were performed using a polarized microscope equipped with a hot stage. Thermal analysis was run on a TA Discovery DSC 2500 using small samples of about 1.0 mg and a heating rate of 10 K min^{-1} under a flow of nitrogen gas. The reported temperatures are transition peak temperatures.

Preparation of pyridinium zwitterions 1[n]a and 1[n]b. A general procedure. A mixture of phenyliodonium derivative **5a** or **5b** [11] (0.20 mmol) and 4-alkoxypyridine[13] (**6[n]**, 1 mL) was stirred for 6 h at 85 °C. All volatiles were removed *in vacuo* (140 °C, 1 mm Hg) and the residue was passed through a silica gel plug (CH_2Cl_2). Alternatively, a solution of **5B** (0.20 mmol) and 4-alkoxypyridine[13] (**6[n]**, 1.0 mmol) in CH_2Cl_2 (0.4 mL) was stirred under argon at 50 °C overnight. Hexane (15 mL) was added to the clear, yellow solution and the mixture was passed through a silica gel plug using CH_2Cl_2/hexane (3:2) to elute the product **1B[n]** and then CH_2Cl_2 to recover the 4-alkoxypyridine (**6[n]**). Crude product **1B[n]** was washed with hot hexane and recrystallized using EtOH/MeCN to give colorless crystals. Analytically pure samples of **1[n]a** and **1[n]b** were obtained by repeated recrystallization from EtOH/MeCN or *iso*-octane/AcOEt giving **1[n]** as white crystalline solids in typical yields of 85-90%.

[*closo*-1-CB_9H_8-10-(NC_5H_4-4-OC_5H_{11})-1-($CH_2CH_2C_6H_4$-4-OAc)] (1A[5]a). Product was obtained in 87% yield (77.6 mg) from [*closo*-1-CB_9H_8-10-IPh-1-($CH_2CH_2C_6H_4$-4-OAc)] (**5Aa**, 0.2 mmol, 96.9 mg): ^{1}H NMR (500 MHz, $CDCl_3$) δ 0.70–2.40 (m, 8H), 0.97 (t, *J* = 7.2 Hz, 3H), 1.39-1.54 (m, 4H), 1.93 (quint, *J* = 7.0 Hz, 2H), 2.31 (s, 3H), 3.32-3.38 (m, 2H), 3.47-3.53 (m, 2H), 4.27 (t, *J* = 6.5 Hz, 2H), 7.06 (d, *J* = 8.4 Hz, 2H), 7.22 (d, *J* = 7.3 Hz, 2H), 7.40 (d, *J* = 8.4 Hz, 2H), 9.09 (d, *J* = 7.3 Hz, 2H); ^{13}C{^{1}H} NMR (126 MHz, $CDCl_3$) δ 14.1, 21.3, 22.4, 28.0, 28.3, 35.2, 38.2, 70.7, 74.5 (br), 112.4, 121.5, 129.6, 140.6, 148.7, 148.8, 169.7, 169.9; ^{11}B NMR (160 MHz, $CDCl_3$) δ –22.0 (d, *J* = 141 Hz, 4B), –17.7 (d, *J* = 154 Hz, 4B), 35.2 (s, 1B); HRMS ESI-TOF(+), *m/z* calcd for $C_{21}H_{34}B_9NO_3K$ $[M+K]^+$: 486.3013, found: 486.3046. Anal. Calcd. for $C_{21}H_{34}B_9NO_3$: C, 56,58; H, 7,69; N, 3.14. Found: C, 56,52; H, 7,48; N, 3.19.

[*closo*-1-CB_9H_8-10-(NC_5H_4-4-OC_7H_{15})-1-($CH_2CH_2C_6H_4$-4-OAc)] (1A[7]a). Product was obtained in 89% yield (84.3 mg) from [*closo*-1-CB_9H_8-10-IPh-1-($CH_2CH_2C_6H_4$-4-OAc)] (**5Aa**, 0.2 mmol, 96.9 mg): ^{1}H NMR (500 MHz, $CDCl_3$) δ 0.75–2.40 (m, 8H), 0.92 (t, *J* = 6.9 Hz, 3H), 1.31-1.37 (m, 4H), 1.40 (quint, *J* = 7.2 Hz, 2H), 1.51 (quint, *J* = 7.5 Hz, 2H), 1.92 (quint, *J* = 7.1 Hz, 2H), 2.31 (s, 3H), 3.32-3.37 (m, 2H), 3.48-3.53 (m, 2H), 4.27 (t, *J* = 6.5 Hz, 2H), 7.05 (d, *J* = 8.4 Hz, 2H), 7.23 (d, *J* = 7.3 Hz, 2H), 7.40 (d, *J* = 8.4 Hz, 2H), 9.09 (d, *J* = 7.3 Hz, 2H); ^{13}C{^{1}H} NMR (126 MHz, $CDCl_3$) δ 14.2, 21.3, 22.7, 25.8, 28.7, 29.0, 31.8, 35.2, 38.2, 70.7, 74.5 (br), 112.4, 121.4, 129.6, 140.6, 148.7, 148.8, 169.7, 169.9; ^{11}B NMR (160 MHz, $CDCl_3$) δ –22.1 (d, *J* = 141 Hz, 4B), –17.7 (d, *J* = 155 Hz, 4B), 35.2 (s, 1B); HRMS ESI-TOF(+), *m/z* calcd for $C_{23}H_{38}B_9NO_3K$ $[M+K]^+$: 514.3326, found: 514.3354. Anal. Calcd. for $C_{23}H_{38}B_9O_3N$: C, 58.30; H, 8.08; N, 2.96. Found: C, 58.09; H, 7.96; N, 3.02.

[*closo*-1-CB_9H_8-10-(NC_5H_4-4-OC_9H_{19})-1-($CH_2CH_2C_6H_4$-4-OAc)] (1A[9]a). Product was obtained in 88% yield (88.3 mg) from [*closo*-1-CB_9H_8-10-IPh-1-($CH_2CH_2C_6H_4$-4-OAc)] (**5Aa**, 0.2 mmol, 96.9 mg): ^{1}H

NMR (500 MHz, $CDCl_3$) δ 0.80–2.40 (m, 8H), 0.90 (t, *J* = 6.9 Hz, 3H), 1.25-1.36 (m, 8H), 1.40 (quint, *J* = 7.0 Hz, 2H), 1.51 (quint, *J* = 7.5 Hz, 2H), 1.92 (quint, *J* = 7.1 Hz, 2H), 2.31 (s, 3H), 3.32-3.37 (m, 2H), 3.48-3.53 (m, 2H), 4.26 (t, *J* = 6.5 Hz, 2H), 7.06 (d, *J* = 8.4 Hz, 2H), 7.22 (d, *J* = 7.3 Hz, 2H), 7.40 (d, *J* = 8.4 Hz, 2H), 9.09 (d, *J* = 7.3 Hz, 2H); $^{13}C\{^1H\}$ NMR (126 MHz, $CDCl_3$) δ 14.2, 21.3, 22.8, 25.9, 28.6, 29.3 (2C), 29.6, 32.0, 35.2, 38.2, 70.7, 74.5 (br), 112.4, 121.5, 129.6, 140.6, 148.7, 148.8, 169.7, 169.9; ^{11}B NMR (160 MHz, $CDCl_3$) δ –22.1 (d, *J* = 141 Hz, 4B), –17.7 (d, *J* = 154 Hz, 4B), 35.2 (s, 1B); HRMS ESI-TOF(+), *m/z* calcd for $C_{25}H_{42}B_9NO_3K$ $[M+K]^+$: 542.3639, found: 542.3669. Anal. Calcd. for $C_{25}H_{42}B_9O_3N$: C, 59.81; H, 8.43; N, 2.79. Found: C, 59.81; H, 8.39; N, 2.83.

[*closo*-1-CB_9H_8-10-(NC_5H_4-4-OC_7H_{15})-1-($CH_2CH_2C_6H_4$-4-OMe)] (1A[7]b). Product was obtained in 88% yield (78.5 mg) from [*closo*-1-CB_9H_8-10-IPh-1-($CH_2CH_2C_6H_4$-4-OMe)] (**5Ab**, 0.2 mmol, 91.3 mg): ^1H NMR (500 MHz, $CDCl_3$) δ 0.75–2.40 (m, 8H), 0.92 (t, *J* = 6.9 Hz, 3H), 1.31-1.37 (m, 4H), 1.40 (quint, *J* = 7.2 Hz, 2H), 1.51 (quint, *J* = 7.8 Hz, 2H), 1.93 (quint, *J* = 7.1 Hz, 2H), 3.27-3.33 (m, 2H), 3.45-3.51 (m, 2H), 3.82 (s, 3H), 4.27 (t, *J* = 6.5 Hz, 2H), 6.90 (d, *J* = 8.6 Hz, 2H), 7.23 (d, *J* = 7.3 Hz, 2H), 7.32 (d, *J* = 8.6 Hz, 2H), 9.10 (d, *J* = 7.3 Hz, 2H); $^{13}C\{^1H\}$ NMR (126 MHz, $CDCl_3$) δ 14.2, 22.7, 25.8, 28.7, 29.0, 31.8, 35.6, 37.9, 55.4, 70.7, 74.9 (br), 112.4, 113.9, 129.5, 135.2, 148.7, 157.8, 169.7; ^{11}B NMR (160 MHz, $CDCl_3$) δ –22.0 (d, *J* = 140 Hz, 4B), –17.8 (d, *J* = 155 Hz, 4B), 35.0 (s, 1B); HRMS ESI-TOF(-), *m/z* calcd for $C_{15}H_{23}B_9NO_2$ $[M-C_7H_{15}]^+$: 348.2566, found: 348.2578. Anal. Calcd. for $C_{22}H_{38}B_9NO_2$: C, 59.27; H, 8.59; N, 3.14. Found: C, 59.19; H, 8.81; N, 3.25.

[*closo*-1-$CB_{11}H_{10}$-12-(NC_5H_4-4-OC_5H_{11})-1-($CH_2CH_2C_6H_4$-4-OAc)] (1B[5]a). Product was obtained from [*closo*-1-$CB_{11}H_{10}$-12-IPh-1-($CH_2CH_2C_6H_4$-4-OAc)] (**5Ba**): ^1H NMR (500 MHz, $CDCl_3$) δ 0.94 (t, *J* = 7.1 Hz, 3H), 1.15–2.70 (m, 10H), 1.34-1.48 (m, 4H), 1.86 (quint, *J* = 7.0 Hz, 2H), 2.12-2.18 (m, 2H), 2.27 (s, 3H), 2.58-2.64 (m, 2H), 4.16 (t, *J* = 6.5 Hz, 2H), 6.94 (d, *J* = 8.5 Hz, 2H), 7.00 (d, *J* = 7.5 Hz, 2H), 7.11 (d, *J* = 8.5 Hz, 2H), 8.46 (d, *J* = 7.5 Hz, 2H); $^{13}C\{^1H\}$ NMR (126 MHz, $CDCl_3$) δ 14.0, 21.2, 22.4, 27.9, 28.3, 36.2, 39.6, 66.4 (br), 70.6, 112.1, 121.4, 129.3, 139.5, 147.6, 148.9, 169.6, 169.7; ^{11}B NMR (160 MHz, $CDCl_3$) δ –14.1 (d, *J* = 144 Hz, 10B), 2.9 (s, 1B); HRMS ESI-TOF(+), *m/z* calcd for $C_{21}H_{37}B_{11}NO_3$ $[M+H]^+$: 472.3797, found: 472.3810. Anal. Calcd. for $C_{21}H_{36}B_{11}NO_3$: C, 53.73; H, 7.73; N, 2.98. Found: C, 53.59; H, 7.61; N, 3.02.

[*closo*-1-$CB_{11}H_{10}$-12-(NC_5H_4-4-OC_7H_{15})-1-($CH_2CH_2C_6H_4$-4-OAc)] (1B[7]a). Product was obtained from [*closo*-1-$CB_{11}H_{10}$-12-IPh-1-($CH_2CH_2C_6H_4$-4-OAc)] (**5Ba**): ^1H NMR (500 MHz, $CDCl_3$) δ 0.89 (t, *J* = 6.9 Hz, 3H), 1.15–2.70 (m, 10H), 1.24-1.39 (m, 6H), 1.45 (quint, *J* = 7.5 Hz, 2H), 1.85 (quint, *J* = 7.1 Hz, 2H), 2.12-2.18 (m, 2H), 2.27 (s, 3H), 2.58-2.64 (m, 2H), 4.16 (t, *J* = 6.5 Hz, 2H), 6.94 (d, *J* = 8.5 Hz, 2H), 7.00 (d, *J* = 7.4 Hz, 2H), 7.11 (d, *J* = 8.5 Hz, 2H), 8.46 (d, *J* = 7.4 Hz, 2H); $^{13}C\{^1H\}$ NMR (126 MHz, $CDCl_3$) δ 14.2, 21.3, 22.7, 25.8, 28.6, 28.9, 31.7, 36.2, 39.6, 66.4 (br), 70.6, 112.1, 121.4, 129.3, 139.4, 147.6, 148.9, 169.6, 169.8; ^{11}B NMR (160 MHz, $CDCl_3$) δ –14.1 (d, *J* = 143 Hz, 10B), 3.1 (s, 1B); HRMS ESI-TOF(+), *m/z* calcd for $C_{23}H_{41}B_{11}NO_3$ $[M+H]^+$: 500.4110, found: 500.4142. Anal. Calcd. for $C_{23}H_{40}B_{11}NO_3$: C, 55.53; H, 8.10; N, 2.82. Found: C, 56.20; H, 7.66; N, 3.05.

[*closo*-1-$CB_{11}H_{10}$-12-(NC_5H_4-4-OC_9H_{19})-1-($CH_2CH_2C_6H_4$-4-OAc)] (1B[9]a). Product was obtained from [*closo*-1-$CB_{11}H_{10}$-12-IPh-1-($CH_2CH_2C_6H_4$-4-OAc)] (**5Ba**): ^1H NMR (500 MHz, $CDCl_3$) δ 0.88 (t, *J* = 7.0 Hz, 3H), 1.15–2.70 (m, 10H), 1.22-1.39 (m, 10H), 1.45 (quint, *J* = 7.4 Hz, 2H), 1.85 (quint, *J* = 7.4 Hz, 2H), 2.12-2.18 (m, 2H), 2.27 (s, 3H), 2.58-2.64 (m, 2H), 4.16 (t, *J* = 6.5 Hz, 2H), 6.94 (d, *J* = 8.5 Hz, 2H), 7.00 (d, *J* = 7.5 Hz, 2H), 7.11 (d, *J* = 8.5 Hz, 2H), 8.46 (d, *J* = 7.4 Hz, 2H); $^{13}C\{^1H\}$ NMR (126 MHz, $CDCl_3$) δ 14.2, 21.3, 22.8, 25.8, 28.6, 29.3, 29.3, 29.5, 31.9, 36.2, 39.6, 66.4 (br), 70.6, 112.1, 121.4, 129.4, 139.4, 147.6, 148.9, 169.6, 169.8; ^{11}B NMR (160 MHz, $CDCl_3$) δ –14.1 (d, *J* = 143 Hz, 10B), 3.0 (s, 1B); HRMS ESI-TOF(+), *m/z* calcd for $C_{25}H_{45}B_{11}NO_3$ $[M+H]^+$: 528.4423, found: 528.4431. Anal. Calcd. for $C_{25}H_{44}B_{11}NO_3$: C, 57.13; H, 8.44; N, 2.67. Found: C, 57.15; H, 8.31; N, 2.72.

[*closo*-1-$CB_{11}H_{10}$-12-(NC_5H_4-4-OC_7H_{15})-1-($CH_2CH_2C_6H_4$-4-OMe)] (1B[7]b). Product was obtained in 86% yield (80.6 mg) from [*closo*-1-$CB_{11}H_{10}$-12-IPh-1-($CH_2CH_2C_6H_4$-4-OMe)] (**5Bb**, 0.2 mmol, 96.0 mg): ^1H NMR (500 MHz, $CDCl_3$) δ 0.89 (t, *J* = 6.8 Hz, 3H), 1.15–2.70 (m, 10H), 1.24-1.40 (m, 6H), 1.45 (quint, *J* = 7.4 Hz, 2H), 1.85 (quint, *J* = 7.0 Hz, 2H), 2.10-2.16 (m, 2H), 2.53-2.59 (m, 2H), 3.76 (s, 3H), 4.16 (t, *J* = 6.5 Hz, 2H), 6.78 (d, *J* = 8.6 Hz, 2H), 7.00 (d, *J* = 7.4 Hz, 2H), 7.03 (d, *J* = 8.6 Hz, 2H), 8.47 (d, *J* = 7.4 Hz, 2H); $^{13}C\{^1H\}$ NMR (126 MHz, $CDCl_3$) δ 14.2, 22.7, 25.8, 28.6, 28.9, 31.8, 35.9, 39.9, 55.4, 66.5 (br s), 70.6, 112.1, 113.8, 129.3, 134.0, 147.6, 157.8, 169.6; ^{11}B NMR (160 MHz, $CDCl_3$) δ –14.2 (d, *J* = 145 Hz, 10B), 3.0 (s, 1B); HRMS ESI(+), *m/z* calcd for $C_{22}H_{41}B_{11}NO_2$ $[M+H]^+$: 472.4161, found: 472.4194; HRMS ESI-TOF(+), *m/z* calcd for $C_{22}H_{40}B_{11}NO_2Na$ $[M+Na]^+$: 494.3980, found: 494.4016. Anal. Calcd. for $C_{22}H_{40}B_{11}NO_2$: C, 56.28; H, 8.59; N, 2.98. Found: C, 56.32; H, 8.77; N, 3.11.

Preparation of sulfonium zwitterions 2A[3]b and 2B[3]b. A general procedure. A solution of crude protected mercaptan **7Ab** or **7Bb** (0.25 mmol) in CH_3CN (18 mL) was treated with $[Me_4N]^+OH^-$•$5H_2O$ (181 mg, 1.00 mmol) and 3-propyl-1,5-dibromopentane[14] (**8**, 67.5 mg, 0.25 mmol). After several minutes, a white precipitate was formed and the reaction mixture was allowed to stir overnight at rt. The reaction mixture was filtered, the filter cake was washed with CH_3CN and the filtrate was evaporated to dryness. The crude material was passed through a SiO_2 plug (CH_2Cl_2) giving sulfonium **2A[3]b** or **2B[3]b** as white crystalline solids in typical yields of 73–77%. Analytically pure samples were obtained by recrystallization from *iso*-octane/AcOEt.

^1H and ^{13}C NMR spectra of **2[3]b** exhibit signals attributed to the *trans* isomer, **2[3]b**-*trans* (major signals) and to the *cis* isomer, **2[3]b**-*cis* (minor isomer) in an approximate ratio of 3:1 for **A** and 5:1 for **B**.

[*closo*-1-CB_9H_8-10-(1-SC_5H_9-4-C_3H_7)-1-($CH_2CH_2C_6H_4$-4-OMe)] (2A[3]b). Product was obtained in 77% yield (76.4 mg) from [*closo*-1-CB_9H_8-10-($SCHNMe_2$)-1-($CH_2CH_2C_6H_4$-4-OMe)] (**7Ab**, 0.25 mmol, 85.7 mg): ^1H NMR (500 MHz, $CDCl_3$) major signals: δ 0.95 (t, *J* = 6.8 Hz, 3H), 0.60–2.50 (m, 8H), 1.33-1.43 (m, 4H), 1.62-1.75 (m, 3H), 2.34 (br d, *J* = 12.3 Hz, 2H), 3.25-3.31 (m, 2H), 3.39 (br t, *J* = 13.0 Hz, 2H), 3.45-3.51 (m, 2H), 3.66 (br d, *J* = 12.8 Hz, 2H), 3.82 (s, 3H), 6.90 (d, *J* = 8.6 Hz, 2H), 7.30 (d, *J* = 8.6 Hz, 2H); minor signals: δ 2.03-2.10 (m), 2.28-2.32 (m), 3.51-3.56 (m); $^{13}C\{^1H\}$ NMR (126 MHz, $CDCl_3$) major signals: δ 14.2, 19.6, 31.1, 35.8, 36.4, 37.7, 38.7, 41.1, 55.4, 86.5 (br), 113.9, 129.5, 134.9, 157.9; minor signals: δ 19.7, 26.6, 33.5, 35.5, 37.1; ^{11}B NMR (160 MHz, $CDCl_3$) major signals: δ -21.1 (d, *J* = 146 Hz, 4B), -16.1 (d, *J* = 156 Hz, 4B), 24.0 (s, 1B); minor signals: δ 22.1 (s, 1B); HRMS ESI-TOF(+), *m/z* calcd for $C_{18}H_{36}B_9OS$ $[M+H]^+$: 399.3324, found: 399.3359. Anal. Calcd. for $C_{18}H_{35}B_9OS$: C, 54.48; H, 8.89; S, 8.08. Found: C, 54.39; H, 9.07; S, 7.79.

[*closo*-1-$CB_{11}H_{10}$-12-(1-SC_5H_9-4-C_3H_7)-1-($CH_2CH_2C_6H_4$-4-OMe)] (2B[3]b). Product was obtained in 73% yield (76.7 mg) from [*closo*-1-$CB_{11}H_{10}$-12-($SCHNMe_2$)-1-($CH_2CH_2C_6H_4$-4-OMe)] (**7Bb**, 0.25 mmol, 91.3 mg): ^1H NMR (500 MHz, $CDCl_3$) major signals: δ 0.89 (t, *J* = 7.2 Hz, 3H), 1.20–2.55 (m, 10H), 1.22-1.27 (m, 2H), 1.29-1.35 (m, 2H), 1.36-1.45 (m, 3H), 2.04-2.09 (m, 2H), 2.17 (br d, *J* = 11.6 Hz, 2H), 2.49-2.54 (m, 2H), 2.77 (br t, *J* = 12.5 Hz, 2H), 3.05 (br d, *J* = 12.3 Hz, 2H), 3.76 (s, 3H), 6.78 (d, *J* = 8.5 Hz, 2H), 7.00 (d, *J* = 8.6 Hz, 2H); minor signals: δ 0.91-0.94 (m), 1.84-1.90 (m), 1.97-2.04 (m), 2.82-2.87 (m), 2.96-3.02 (m); $^{13}C\{^1H\}$ NMR (151 MHz, $CDCl_3$) major

signals: δ 14.2, 19.5, 30.7, 35.6, 35.6, 38.2, 38.6, 40.7, 55.4, 72.7 (br s), 113.8, 129.3, 133.7, 157.9; minor signals: δ 20.0, 26.7, 32.7; ^{11}B NMR (160 MHz, $CDCl_3$) δ –14.7 (d, *J* = 145 Hz, 5B), -13.4 (d, *J* = 168 Hz, 5B), -5.9 (s, 1B); HRMS ESI-TOF(+), *m/z* calcd for $C_{18}H_{38}B_{11}OS$ $[M+H]^+$: 423.3667, found: 423.3701. Anal. Calcd. for $C_{18}H_{37}B_{11}OS$: C, 51.42; H, 8.87; S, 7.63. Found: C, 51.14; H, 8.96; S, 7.49.

Preparation of esters 3A[7]b and 4A[3]b. A General procedure. According to a general literature procedure,[9] a solution of carboxylic acid **9A[7]** [7,12] or **10A[3]** [9,16] (0.50 mmol) was dissolved in anhydrous CH_2Cl_2 (5 mL). $(COCl)_2$ (0.064 mL, 0.75 mmol) and a catalytic amount of *N,N*-dimethylformamide were added, the reaction mixture was stirred for 1 h, and volatiles were removed *in vacuo*. The residue was dissolved in dry CH_2Cl_2 (5 mL) and Et_3N (0.418 mL, 3.00 mmol) and 4-methoxyphenol (95.6 mg, 0.77 mmol) were added. The reaction was stirred overnight at ambient temperature. The reaction mixture was washed with 5% HCl, organic layer dried (Na_2SO_4), and solvent was removed. The crude material was passed through a silica gel plug (CH_2Cl_2/hexane, gradient 4:1 to 1:1) giving esters **3A[7]b** and **4A[3]b** as white crystalline solids in typical yields of 57–61%. Analytically pure samples were obtained by recrystallization from *iso*-octane/AcOEt.

[*closo*-1-CB_9H_8-10-(NC_5H_4-4-OC_7H_{15})-1-($COOC_6H_4$-4-OMe)] (3A[7]b). Product was obtained in 61% yield (141 mg) from [*closo*-1-CB_9H_8-10-(NC_5H_4-4-OC_7H_{15})-1-COOH] (**9A[7]**,[7,12] 0.50 mmol, 170 mg): ^{1}H NMR (500 MHz, $CDCl_3$) δ 0.75–2.85 (m, 8H), 0.91 (t, *J* = 6.9 Hz, 3H), 1.29-1.35 (m, 4H), 1.39 (quint, *J* = 7.1 Hz, 2H), 1.50 (quint, *J* = 7.5 Hz, 2H), 1.91 (quint, *J* = 7.1 Hz, 2H), 3.83 (s, 3H), 4.28 (t, *J* = 6.5 Hz, 2H), 6.95 (d, *J* = 9.0 Hz, 2H), 7.27 (d, *J* = 8.6 Hz, 4H), 9.05 (d, *J* = 7.4 Hz, 2H); ^{13}C{^{1}H} NMR (126 MHz, $CDCl_3$) δ 14.2, 22.7, 25.8, 28.6, 29.0, 31.8, 55.8, 68.3 (br s), 70.9, 112.6, 114.5, 122.7, 145.2, 148.4, 157.3, 168.9, 170.2; ^{11}B NMR (160 MHz, $CDCl_3$) δ –21.3 (d, *J* = 140 Hz, 4B), –16.3 (d, *J* = 155 Hz, 4B), 41.6 (s, 1B); HRMS ESI-TOF(-), *m/z* calcd for $C_{14}H_{19}B_9NO_4$ $[M\text{-}C_7H_{15}]^+$: 364.2152, found: 364.2166. Anal. Calcd. for $C_{21}H_{34}B_9O_4N$: C, 54,62; H, 7.42; N, 3.03. Found: C, 54.49; H, 7.53; N, 3.08.

[*closo*-1-CB_9H_8-10-(SC_5H_9-4-C_3H_7)-1-($COOC_6H_4$-4-OMe)] (4A[3]b). Product was obtained in 57% yield (118 mg) from [*closo*-1-CB_9H_8-10-(SC_5H_9-4-C_3H_7)-1-COOH] [9,16] (**10A[3]**, 0.50 mmol, 153 mg): ^{1}H NMR (500 MHz, $CDCl_3$) major signals: δ 0.94 (t, *J* = 6.9 Hz, 3H), 0.60–2.80 (m, 8H), 1.33-1.43 (m, 4H), 1.65-1.77 (m, 3H), 2.36 (br d, *J* = 14.1 Hz, 2H), 3.41 (br t, *J* = 13.1 Hz, 2H), 3.69 (br d, *J* = 12.8 Hz, 2H), 3.83 (s, 3H), 6.96 (d, *J* = 9.0 Hz, 2H), 7.26 (d, *J* = 9.0 Hz, 2H); minor signals: δ 2.05-2.13 (m), 2.25-2.32 (m), 3.51-3.58 (m); ^{13}C{^{1}H} NMR (126 MHz, $CDCl_3$) major signals: δ 14.2, 19.6, 31.0, 35.8, 38.6, 41.0, 55.7, 78.8 (br), 114.5, 122.6, 145.1, 157.4, 167.7; minor signals: δ 19.7, 26.6, 33.3, 35.4, 37.0; ^{11}B NMR (160 MHz, $CDCl_3$) major signals: δ -20.3 (d, *J* = 147 Hz, 4B), -14.7 (d, *J* = 161 Hz, 4B), 31.1 (s, 1B); minor signal: δ 29.4 (s, 1B); HRMS ESI-TOF(+), *m/z* calcd for $C_{17}H_{32}B_9O_3S$ $[M+H]^+$: 415.2910, found: 415.2937. Anal. Calcd. for $C_{17}H_{31}B_9O_3S$: C, 49.46; H, 7.57; S, 7.77. Found: C, 49.59; H, 7.51; S, 7.83.

Preparation of protected mercaptans 7Ab and 7Bb. **A general procedure.** Following a general literature procedure[17], a solution of phenyliodonium zwitterion **5Ab** or **5Bb** (0.30 mmol) in freshly distilled *N,N*-dimethylthioformamide (0.60 mL) was stirred at 100 °C for 1 hr. Excess *N,N*-dimethylthioformamide was removed using short path distillation (Kugel-Rohr, 100 °C, 1.0 mmHg) and the resulting residue was washed with hexane to remove the remaining *N,N*-dimethylthioformamide. The crude product was passed through a short silica gel plug (CH_2Cl_2) giving protected mercaptans **7Ab** or **7Bb** as off-white solids in typical yields 90-98%, which were used in the next without further purification.

[*closo*-1-CB_9H_8-10-($SCHNMe_2$)-1-($CH_2CH_2C_6H_4$-4-OMe)] (7Ab). Product was obtained in 98% yield (101 mg) from [*closo*-1-CB_9H_8-10-IPh-1-($CH_2CH_2C_6H_4$OMe-4)] (**5Ab**, 0.3 mmol, 137 mg): mp 195-196 °C;^{1}H NMR (200 MHz, $CDCl_3$) δ 0.45–2.60 (m, 8H), 3.22-3.34 (m, 2H), 3.39-3.51 (m, 2H), 3.58 (s, 3H), 3.65 (s, 3H), 3.82 (s, 3H), 6.89 (d, *J* = 8.5 Hz, 2H), 7.30 (d, *J* = 8.5 Hz, 2H), 9.69 (s, 1H); ^{13}C{^{1}H} NMR (126 MHz, $CDCl_3$) δ 36.1, 37.8, 41.6, 48.8, 55.4, 80.2 (br), 113.9, 129.5, 135.1, 157.8, 187.6; ^{11}B NMR (160 MHz, $CDCl_3$) δ –21.0 (d, *J* = 142 Hz, 4B), –16.6 (d, *J* = 155 Hz, 4B), 26.5 (s, 1B); HRMS ESI-TOF(+), *m/z* calcd for $C_{13}H_{27}B_9NOS$ $[M+H]^+$: 344.2651, found: 344.2667.

[*closo*-1-$CB_{11}H_{10}$-12-($SCHNMe_2$)-1-($CH_2CH_2C_6H_4$-4-OMe)] (7Bb). Product was obtained in 90% yield (98.6 mg) from [*closo*-1-$CB_{11}H_{10}$-12-IPh-1-($CH_2CH_2C_6H_4$-4-OMe)] (**5Bb**, 0.3 mmol, 96.0 mg): mp 213-214 °C; ^{1}H NMR (500 MHz, $CDCl_3$) δ 1.15–2.70 (m, 10H), 2.03-2.12 (m, 2H), 2.49-2.57 (m, 2H), 3.34 (s, 3H), 3.56 (s, 3H), 3.76 (s, 3H), 6.77 (d, *J* = 8.0 Hz, 2H), 7.01 (d, *J* = 8.0 Hz, 2H), 9.01 (s, 1H); ^{13}C{^{1}H} NMR (126 MHz, $CDCl_3$) δ 35.7, 40.4, 41.6, 48.8, 55.4, 69.7 (br), 113.8, 129.3, 134.0, 157.8, 186.6; ^{11}B NMR (160 MHz, $CDCl_3$) δ –13.5 (d, *J* = 145 Hz, 10B), -4.6 (s, 1B); HRMS ESI-TOF(-) *m/z* calcd for $C_{12}H_{25}B_{11}NOS$ $[M\text{-}Me]^+$: 352.2680, found: 352.2697.

Binary mixtures preparation. Solutions of derivatives **1**–**4** in **ClEster** host (15–20 mg of the host) were prepared in open vials. The mixtures in CH_2Cl_2 were heated for 2 hr at 60 °C to remove the solvent. They were analyzed by polarized optical microscopy (POM) to ensure their homogeneity. The mixtures were then allowed to stand for 2 hr at room temperature before conducting thermal and dielectric measurements.

Dielectric measurements. Dielectric properties of solutions of **1**–**4** in **ClEster** were measured by a Liquid Crystal Analytical System (LCAS - Series II, LC Vision, Inc.) using GLCAS software version 0.13.14, which implements literature procedures for dielectric constants. The homogenous binary mixtures were loaded into ITO electro-optical cells by capillary forces with moderate heating supplied by a heat gun. The cells (12 μm thick, electrode area 1.00 cm^2, and anti-parallel rubbed polyimide layer) were obtained from LC Vision, Inc. The filled cells were heated to an isotropic phase and cooled to room temperature before measuring dielectric properties. Default parameters were used for measurements: triangular shaped voltage bias ranging from 0.1–20 V at 1 kHz frequency. The threshold voltage V_{th} was measured at a 5% change. For each mixture the measurement was repeated 10 times for two independent cells. The results were averaged to calculate the mixture's parameters and are tabularized in the ESI. The electrical resistivity of the mixtures was measured in the electrooptical cells at about 1×10^{11} ohm cm. All measurements were run at 22 °C. Error in concentration is estimated at about 1.5%. The dielectric values obtained for each concentration were compared to values for the pure host measured in a 4 μm thick cell and homeotropic alignment. The resulting extrapolated values for pure additives are shown in Table 5. The dielectric data was analyzed using the Maier-Meier formalism as described previously.[9,39]

Conflicts of interest

There are no conflicts to declare.

Acknowledgements

This work was supported by the Foundation for Polish Science (TEAM/2016-3/24), NSF (DMR-1611250) and NCN (OPUS 2015/17/B/ST5/02801) grants. We thank Prof. P. Kula for the gift of **ClEster**.

Notes and references

1 P. Kaszynski In *Handbook of Boron Science*; Hosmane, N. S., Eagling, R., Eds.; World Scientific: London, 2018; Vol. 3, p 57-114.

2 S. Naemura, in *Physical Properties of Liquid Crystals: Nematics*, (Eds.: D. A. Dunmur, A. Fukuda, and G. R. Luckhurst) IEE, London, **2001**, pp 523-581.

3 P. Kirsch, M. Bremer, *Angew. Chem., Int. Ed.,* 2000, **39**, 4216-4235.

4 D. Pauluth, K. Tarumi, *J. Mater. Chem.,* 2004, **14**, 1219-1227.

5 S. Urban, in *Physical Properties of Liquid Crystals: Nematics*, (Eds.: D. A. Dunmur, A. Fukuda, and G. R. Luckhurst) IEE, London, **2001**, pp 267-276.

6 a) L. M. Blinov, in *Handbook of Liquid Crystals*, *Vol. 1* (Eds.: D. Demus, J. W. Goodby, G. W. Gray, H.-W. Spiess, V. Vill), Wiley-VCH, New York, **1998**, pp. 477-534; b) L. M. Blinov, V. G. Chigrinov, *Electrooptic Effects in Liquid Crystal Materials*, Springer-Verlag, New York, **1994**.

7 B. Ringstrand, P. Kaszynski, *J. Mater. Chem.,* 2010, **20**, 9613-9615.

8 B. Ringstrand, P. Kaszynski, *J. Mater. Chem.,* 2011, **21**, 90-95.

9 J. Pecyna, P. Kaszyński, B. Ringstrand, M. Bremer, *J. Mater. Chem. C,* 2014, **2**, 2956-2964.

10 J. Pecyna, R. P. Denicola, H. M. Gray, B. Ringstrand, P. Kaszynski, *Liq Cryst,* 2014, **41**, 1188-1198.

11 R. Jakubowski, A. Pietrzak, A. C. Friedli, P. Kaszyński, *Chem. Eur. J.,* 2020, **26**, 17481–17494.

12 P. Kaszynski, B. Ringstrand, *Angew. Chem. Int. Ed.,* 2015, **54**, 6576-6581.

13 A. N. Hajhussein, L. S. Abuzahra, A. Pietrzak, M. F. Sadek, M. O. Ali, J. Wojciechowski, A. C. Friedli, P. Kaszyński, *Arkivoc,* 2018, 225 - 235.

14 B. Ringstrand, M. Oltmanns, J. A. Batt, A. Jankowiak, R. P. Denicola, P. Kaszynski, *Beilstein J. Org. Chem.,* 2011, **7**, 386-393.

15 B. Ringstrand, P. Kaszynski, A. Januszko, V. G. Young, Jr., *J. Mater. Chem.,* 2009, **19**, 9204-9212.

16 J. Pecyna, R. P. Denicola, B. Ringstrand, A. Jankowiak, P. Kaszynski, *Polyhedron,* 2011, **30**, 2505-2513.

17 J. Pecyna, R. Żurawiński, P. Kaszyński, D. Pociecha, P. Zagórski, S. Pakhomov, *Eur. J. Inorg. Chem.,* 2016, 2923-2931.

18 A. Franken, M. J. Carr, W. Clegg, C. A. Kilner, J. D. Kennedy, *Dalton Trans.,* 2004, 3552-3561.

19 M. J. Carr, A. Franken, R. Macias, J. D. Kennedy, *Polyhedron,* 2006, **25**, 1069-1075.

20 A. S. Larsen, J. D. Holbrey, F. S. Tham, C. A. Reed, *J. Am. Chem. Soc.,* 2000, **122**, 7264-7272.

21 B. Ringstrand, P. Kaszynski, V. G. Young, Jr., Z. Janoušek, *Inorg. Chem.,* 2010, **49**, 1166-1179.

22 R. Zurawinski, R. Jakubowski, S. Domagała, P. Kaszyński, K. Woźniak, *Inorg. Chem.,* 2018, **57**, 10442−10456.

23 J. Pecyna, B. Ringstrand, S. Domagała, P. Kaszyński, K. Woźniak, *Inorg. Chem.,* 2014, **53**, 12617-12626.

24 P. Tokarz, P. Kaszyński, S. Domagała, K. Woźniak, *J. Organomet. Chem.,* 2015, **798**, 70-79.

25 M. O. Ali, D. Pociecha, J. Wojciechowski, I. Novozhilova, A. C. Friedli, P. Kaszyński, *J. Organometal. Chem.,* 2018, **865**, 226-233.

26 A. Jankowiak, A. Balinski, J. E. Harvey, K. Mason, A. Januszko, P. Kaszynski, V. G. Young, Jr., A. Persoons, *J. Mater. Chem. C,* 2013, **1**, 1144-1159.

27 M. O. Ali, J. C. Lasseter, R. Żurawiński, A. Pietrzak, J. Pecyna, J. Wojciechowski, A. C. Friedli, D. Pociecha , P. Kaszyński, *Chem. Eur. J.,* 2019, **25**, 2616–2630.

28 D. Demus In *Handbook of Liquid Crystals*; Demus, D., Goodby, J. W., Gray, G. W., Spiess, H.-W., Vill, V., Eds.; Wiley-VCH: New York, 1998; Vol. 1, p 133-187.

29 T. Nagamine, A. Januszko, K. Ohta, P. Kaszynski, Y. Endo, *Liq. Cryst.,* 2008, **35**, 865-884.

30 R. Dabrowski, J. Jadzyn, J. Dziaduszek, Z. Stolarz, G. Czechowski, M. Kasprzyk, *Z. Naturforsch.,* 1999, **54a**, 448-452.

31 S. Urban, J. Kędzierski, R. Dąbrowski, *Z. Naturforsch.,* 2000, **55a**, 449–456.

32 For details see the Electronic Supplementary Information.

33 W. Maier, G. Meier, *Z. Naturforsch.,* 1961, **16A**, 262-267 and 470-477.

34 A. Januszko, K. L. Glab, P. Kaszynski, K. Patel, R. A. Lewis, G. H. Mehl, M. D. Wand, *J. Mater. Chem.,* 2006, **16**, 3183–3192.

35 R. Dabrowski, J. Jadżyn, S. Czerkas, J. Dziaduszek, A. Walczak, *Mol. Cryst. Liq. Cryst.,* 1999, **332**, 61-68.

36 M. J. Frisch, G. W. Trucks, H. B. Schlegel, G. E. Scuseria, M. A. Robb, J. R. Cheeseman, G. Scalmani, V. Barone, B. Mennucci, G. A. Petersson, H. Nakatsuji, M. Caricato, X. Li, H. P. Hratchian, A. F. Izmaylov, J. Bloino, G. Zheng, J. L. Sonnenberg, M. Hada, M. Ehara, K. Toyota, R. Fukuda, J. Hasegawa, M. Ishida, T. Nakajima, Y. Honda, O. Kitao, H. Nakai, T. Vreven, J. A. Montgomery, Jr., J. E. Peralta, F. Ogliaro, M. Bearpark, J. J. Heyd, E. Brothers, K. N. Kudin, V. N. Staroverov, R. Kobayashi, J. Normand, K. Raghavachari, A. Rendell, J. C. Burant, S. S. Iyengar, J. Tomasi, M. Cossi, N. Rega, J. M. Millam, M. Klene, J. E. Knox, J. B. Cross, V. Bakken, C. Adamo, J. Jaramillo, R. Gomperts, R. E. Stratmann, O. Yazyev, A. J. Austin, R. Cammi, C. Pomelli, J. W. Ochterski, R. L. Martin, K. Morokuma, V. G. Zakrzewski, G. A. Voth, P. Salvador, J. J. Dannenberg, S. Dapprich, A. D. Daniels, O. Farkas, J. B. Foresman, J. V. Ortiz, J. Cioslowski, and D. J. Fox, Gaussian 09, Revision A.02, Gaussian, Inc., Wallingford CT, 2009.

37 M. Cossi, G. Scalmani, N. Rega, V. Barone, *J. Chem. Phys.,* 2002, **117**, 43-54 and references therein.

38 G. R. Fulmer, A. J. M. Miller, N. H. Sherden, H. E. Gottlieb, A. Nudelman, B. M. Stoltz, J. E. Bercaw, K. I. Goldberg, *Organometallics,* 2010, **29**, 2176–2179.

39 P. Kaszynski, A. Januszko, K. L. Glab, *J. Phys. Chem. B,* 2014, **118**, 2238-2248.

Graphical TOC